International Journal of Coal Geology 195 (2018) 37–46

Contents lists available at ScienceDirect

International Journal of Coal Geology

journal homepage: www.elsevier.com/locate/coal

Scale effects and strength anisotropy in coal

Honghua Song[a,d,*], Yaodong Jiang[b,c], Derek Elsworth[d], Yixin Zhao[a,c,d,*], Jiehao Wang[d], Bin Liu[a]

[a] College of Resources and Safety Engineering, China University of Mining and Technology, Beijing, China
[b] School of Mechanics and Civil Engineering, China University of Mining and Technology, Beijing 100083, China
[c] State Key Laboratory of Coal Resources and Safe Mining, China University of Mining and Technology, Beijing 100083, China
[d] Energy and Mineral Engineering, G3 Center and EMS Energy Institute, Pennsylvania State University, University Park, PA, USA

ARTICLE INFO

Keywords:
Coal
Scale effect
Strength anisotropy
Computed tomography
Microstructure

ABSTRACT

We explore microstructure-related effects of loading direction and specimen size on the anisotropy of uniaxial compressive strength in coal. We measure uniaxial compressive strength on coal samples of four different diameters (25 to 75 mm) and with varied dip of the bedding plane with respect to loading direction (0°, 15°, 30°, 45°, 60° and 90°) including characterizing the variation of microstructures in the specimens by X-ray imaging. The uniaxial compressive strength for each specimen size exhibits a unique U-shape curve against the angle of anisotropy (Jaeger, 1971). The degree of the strength anisotropy decreases with increasing specimen size, principally due to the enhanced microstructural volume of a larger specimen. The contribution of microstructures on uniaxial compressive strength differs for different orientations of loading relative to anisotropy. The rate of decline of the average uniaxial compressive strength with increasing specimen size is greatest when loading is parallel to bedding (anisotropic angle of 0°) and is the most moderate at 45°. An empirical equation relating specimen diameter with uniaxial compressive strength is proposed and verified against the experimental data. Based on this equation, the UCS of coal samples with different orientations relative to the anisotropy are predicted for the limiting sizes of zero and ∞. The anisotropy of the scale effect is also explored. Meanwhile, it is verified that a cosine relation between anisotropy angle and uniaxial compressive strength is applicable to coal specimens of different sizes. This demonstrates that the strength anisotropy in coal will remain constant when the specimen diameter is larger than a critical threshold. Based on these two observations/equations, a universal equation relying on the minimum strength angle, friction angle and Weibull coefficients is proposed and verified against experimental data to describe the relationship among anisotropy angle, specimen size, and uniaxial compressive strength in coal.

1. Introduction

Coal is a naturally discontinuous, inhomogeneous, and anisotropic material. The uniaxial compressive strength (UCS) of coal is significantly influenced by sample size and microstructures, including the presence of mineral inclusions and pre-existing cracks (Protodiakonov and Koifman, 1963; Wagner, 1974). Understanding the mechanical anisotropy of coal related to scale effects and the role of interior microstructures is the key in upscaling laboratory experimental data to field scale. These needs are important in interpreting in-situ stress measurements (Amadei, 1996; Medhurst, 1997), coal pillar design (Medhurst and Brown, 1998), roadway support and geological evolution of rock masses (Levine and Davis, 1984).

In unraveling the impact of microstructures on the macroscopic mechanical properties of coal, strength anisotropy is known to be controlled by the degree of cleating and the brightness of coal (Medhurst and Brown, 1998; Pan et al., 2013; Poulsen and Adhikary, 2013), the distribution and the occurrence of mineral inclusions (Gao et al., 2014; Zhao et al., 2014a, 2014b), and the volume variation of these microstructures (Scholtès et al., 2011). These factors increase the heterogeneity of coal samples. Simultaneously, varied distributions of these microstructures, formed in the sedimentation and coalification process (Cai et al., 2015; Pan et al., 2016; Ward, 2016), may contribute to the continuous variation of mechanical properties in coal including the UCS (Okubo et al., 2006; Pomeroy et al., 1971), dynamic indirect tensile strength (Zhao et al., 2014a, 2014b), and dynamic fracture toughness (Zhao et al., 2017). However, the relation between strength anisotropy and the distribution of microstructures in coal is not well understood, nor constrained.

Scale effects relate the dependence of the UCS to the sample size but they are also manifest in the strength anisotropy of coal, as the increasing density of pre-existing micro-cracks with specimen size

* Corresponding authors at: College of Resources and Safety Engineering, China University of Mining and Technology, Beijing, China.
E-mail addresses: honghuasong8@hotmail.com (H. Song), zhaoyx@cumtb.edu.cn (Y. Zhao).

https://doi.org/10.1016/j.coal.2018.05.006
Received 19 March 2018; Received in revised form 17 May 2018; Accepted 17 May 2018
Available online 18 May 2018

enhances the potential for coal failure (Bieniawski, 1968a, 1968b; George, 1997; Weibull, 1939). However, due to difficulties in processing coal specimens of different sizes and angles of intrinsic anisotropy (angles between drilling or loading direction and the orientation of bedding plane), the effect of specimen size and loading direction (strength anisotropy) of coal is still not fully understood. Previous explanations of the scale effect are not related to the occurrence and variation of mineral inclusions (Cai et al., 2015). X-ray computed tomography (X-ray CT) is a nondestructive imaging technique (Karpyn and Piri, 2007; Van Belleghem et al., 2016; Vogel et al., 2005) which may be applied in the characterization of cleats/fractures, minerals distribution, and gas sorption properties in coal (Karacan and Okandan, 2001; Liu et al., 2017; Mao et al., 2015; Shi et al., 2018; Vega et al., 2014). It is capable of providing quantitative characterization of the interior structure of materials, including the distribution and volume variation of microstructures in coal with the specimen size.

We explore the influence of loading direction and specimen size on uniaxial compressive strength using coal samples with four different diameters (25 to 75 mm) and varied dip of the bedding with respect to loading direction (0°, 15°, 30°, 45°, 60° and 90°). X-ray CT is used to characterize the distribution and volume of microstructures varying with specimen size and loading direction to reveal the dependence of scale effect and strength anisotropy on microstructures in coal.

2. Theoretical background

A variety of empirical equations have related UCS to specimen size and anisotropy. These are critically reviewed to understand mechanisms of characterizing scale effect and strength anisotropy in coal and rock.

2.1. Scale effect

The relationship between specimen size and strength in rock material has been experimentally and numerically investigated (Brook, 1985; Cundall et al., 2008; Gregory and Herbert, 1981; Hoek and Brown, 1997; Mas Ivars et al., 2008; Masoumi et al., 2015; Qi et al., 2014), empirical equations are proposed. Such relations may be based on statistical models of specimen size and the UCS (Weibull, 1939, 1951) as

$$m \log \frac{\sigma_1}{\sigma_2} = \log \frac{V_1}{V_2} \tag{1}$$

where σ_1 and σ_2 are the UCS of separate specimens of volume V_1 and V_2, respectively; m is a constant representing the slope of Eq. (1). However, Eq. (1) cannot be used in coal, as the relationship between $\log(\sigma_1/\sigma_2)$ and $\log(V_1/V_2)$ is not linear (Bieniawski, 1968a).

An alternative is (Protodiakonov and Koifman, 1963),

$$\sigma_d = \frac{d + mb}{d + b}\sigma_M \tag{2}$$

where σ_d is the strength of a cubical rock specimen of side length d; $m = \sigma_0/\sigma_M$ is a constant with σ_M representing the strength of the rock mass, namely as $d \to \infty$, and σ_0 is the strength of the specimen with $d \to 0$; b is the spacing of the discontinuities in the rock mass. The formula illustrates the decrease in UCS with increasing specimen size with the UCS is bounded by a constant when $d \to \infty$. However, the physical meaning of b in Eq. (2) is not logically defined, as the specimen size $d < b$.

Bieniawski (1968b) proposed approximate empirical equations to appropriately describe the relationship between specimen size and the UCS of coal. The empirical relationships between specimen size and uniaxial compressive strength for the coal specimen and mass, are respectively,

$$\sigma = 1100\frac{w^{0.16}}{h^{0.55}} \tag{3}$$

$$\sigma = 400 + 220\frac{w}{h} \tag{4}$$

where σ is the specimen strength; w is the pillar width; h is the pillar height. These two equations indicate that the UCS of coal is affected by the specimen shape and size, and the UCS in a coal mass depends on the shape of the coal mass. However, this relation has a difficulty in defining what sizes are appropriate for each expression.

Based on the analysis of the published data from different rock types, a universal relation was proposed by Hoek and Brown (1980) to predict the scale effect in the uniaxial compressive testing of rocks as

$$\sigma_d = \sigma_{50}\left(\frac{50}{d}\right)^{0.18} \tag{5}$$

where σ_{50} is the UCS of a 50 mm diameter sample; σ_d is the related UCS of the specimen whose diameter is d mm. Although this equation illustrates that the UCS and specimen size have an (negative) exponential dependency, it cannot reproduce a reasonable constant σ_d as $d \to \infty$.

2.2. Strength anisotropy

Anisotropic strength properties have also been broadly investigated for various sedimentary rocks (Chenevert and Gatlin, 1965; McLamore and Gray, 1967; Pietruszczak et al., 2002), including sandstones (Al-Harthi, 1998; Jing et al., 2002; Khanlari et al., 2015), shales (Heng et al., 2015), mudstones (Ajalloeian and Lashkaripour, 2000) and schists (Behrestaghi et al., 1996; Deklotz et al., 1966; Nasseri et al., 2003). A review of these indicates that the failure strength is a maximum either when the dip is $\beta = 0°$ or 90°, and the lowest failure strength is reached as $\beta = 45° - \varphi/2$, where β is the inclination of anisotropy (between the loading direction and the foliation plane) and φ is the friction angle along the plane of weakness. Three groups of anisotropic behavior were classified by Ramamurthy (1993), namely U-type, undulatory-type and shoulder-type.

Empirical relationships between the loading direction and rock strength have also been investigated, under both uniaxial and triaxial compressive loading conditions (Cho et al., 2012; Nasseri et al., 2003b; Pomeroy et al., 1971; Rafiai, 2011; Saeidi et al., 2013; Saroglou and Tsiambaos, 2008). The most commonly used equation relating the direction anisotropy of rock strength in the uniaxial loading condition (Donath, 1961; Jaeger, 1960) is

$$\sigma_\beta = A - D\cos 2(\beta - \beta_{\min}) \tag{6}$$

where σ_β is the UCS at anisotropic angle of β; β is the bedding plane orientation relative to the maximum loading direction; β_{min} is the anisotropy angle where the UCS is minimum; A and D are constants relating to the friction angle of coal and defining the UCS relative to the degree of strength anisotropy. This equation is only applicable to anisotropic strength curves with a U-shaped form.

3. Material and methods

A series of different-sized coal samples are prepared with different inclinations of anisotropy. Interior structure is obtained via X-ray CT and strength measured under uniaxial confinement.

3.1. Properties of coal

The coal blocks used in this experiment were excavated from the No. 45 coal seam in the Wudong Mine, Xinjiang Province, China. The water-polycrylic resin was wrapped on the block surfaces immediately after recovery from the working face, to prevent oxidation and drying during transportation. The density of the coal is ~1.46 g/cm^3, and the moisture content is ~1.8%. Mineral matter is present only in minor

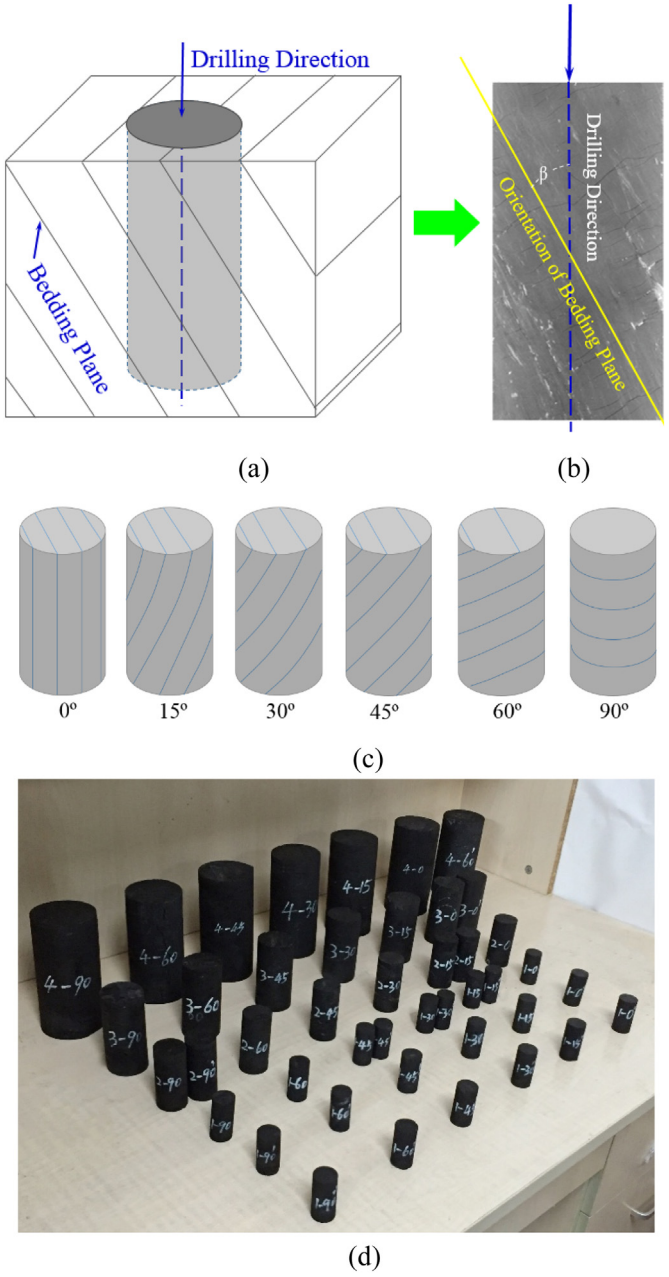

Fig. 1. Specimen process: (a) Schematic of coal blocks after trimming; (b) The anisotropic angle (β) between drilling direction and orientation of bedding plane; (c) Schematic of specimens with different anisotropic angles in each group; (d) Part of the specimen in each group used in this experiment.

proportions (8.2%), comprising kaolinite (62.0%), nacrite (26.5%), lizardite (10.8%), and pentahydroborite (0.4%). These proportions are measured by X-ray diffraction (XRD).

3.2. Specimen preparation

The coal blocks are trimmed to square the specimens, as shown in Fig. 1(a), then they are processed according to the standards recommended by ISRM. Four groups of coal specimens with length to diameter ratio of 2 and diameters of 25 mm, 38 mm, 50 mm, and 75 mm are drilled from the block samples. For each group of coal specimens, angles between the drilling direction and the orientations of the bedding plane are chosen as 0°, 15°, 30°, 45°, 60°, and 90°, as shown in Fig. 1(b) and (c).

3.3. Micro-xCT scanning

To obtain the distribution and volume variation of microstructures relative to the loading direction, six specimens were scanned before the test. Five of these specimens have a diameter of 50 mm and anisotropic angles of 0°, 30°, 45°, 60°, and 90° are used to investigate the microstructure variation in each orientation, and another specimen with a diameter of 75 mm and anisotropic angle of 45° is used to study the volume variation of microstructures with a change in specimen size. The X-ray micro CT imaging is by NanoVoxel 4000 (Sanying, China) with a high voltage X-ray source (225 kV, 240 kV and 300 kV optional), and sub-micron spatial resolution ($\leq$0.5 μm). The voltage used here is 225 kV to yield a spatial resolution of 0.5 μm.

3.4. Uniaxial compression test

Uniaxial compression tests (ISRM, 2007) are conducted on a load frame with 100kN capacity and a precision of ± 0.5%. The tests are at room temperature and under displacement-control at 1 mm/min.

4. Result and discussion

4.1. CT scanning

Fig. 2 shows cross sections of samples with angles of anisotropy of 0°, 30°, 45°, 60°, and 90°. It is apparent that microstructures including mineral inclusions and pre-existing cracks are present throughout these coal specimens. Mineral inclusions are unevenly distributed along the bedding plane and exhibit a zonal shape. Bedding plane cracks are usually parallel to the bedding plane. Primary cleats are approximately perpendicular to the bedding plane – these primary cleats are greater in quantity, have a shorter length and are more intense than secondary cleats, as shown in Fig. 2(c). Random cleats are randomly distributed in the coal specimen. The crack length of random cleats is usually longer than other cleats, although they have a lower fracture density. Meanwhile, the angle between the loading direction and the orientation of the primary cleats decreases, as the angle of anisotropy increases.

To investigate the volume variation of mineral inclusion and pre-existing cracks as coal specimen size increases, three groups of specimens with height to width ratio of 2 and diameters of 25 mm, 38 mm, and 50 mm are cut from a single 75 mm diameter specimen with an anisotropic angle of 45°, scanned by X-ray CT.

Each group was cropped from a corner and enlarged to the middle of the specimen, to ensure microstructures with consistent features, as indicated in Fig. 3(a). Group A and their corresponding parts in the X-ray CT images are shown in Fig. 3(b). The cropping process for groups B and C are the same as for group A, except that they begin from corners B and C, respectively. Meanwhile, the volume of mineral inclusions and pre-existing cracks in group A, B, and C are also calculated (Table 1).

The volume of mineral inclusions and pre-existing cracks increase with the specimen size. As the specimen diameter increases from 25 mm to 50 mm, the average volume of initial cracks and mineral inclusions increases from 14.52 mm^3 and 219.31 mm^3 to 185.48 mm^3 and 476.92 mm^3, respectively. However, the volume variation of mineral inclusions decreases from 104.30% to 83.80%, and the variation of pre-existing cracks reduces from 97.49% to 48.49%. Meanwhile, the average volume and volume variation of mineral inclusions in various specimen sizes are larger than that of pre-existing cracks.

In addition, bedding plane features (length, density, etc.) may also influence the anisotropy (fracture feature, strength, etc.) of coal at different scales. However, due to the only slight difference in gray-scale value between the coal matrix and bedding planes, the interfaces are not readily recovered from the X-ray CT images. As shown in Fig. 2, these data cannot give a quantitative measurement of bedding planes (length, density, etc.) in coal, despite many attempts. This is in contrast to other stratified rocks where the density difference between bedding

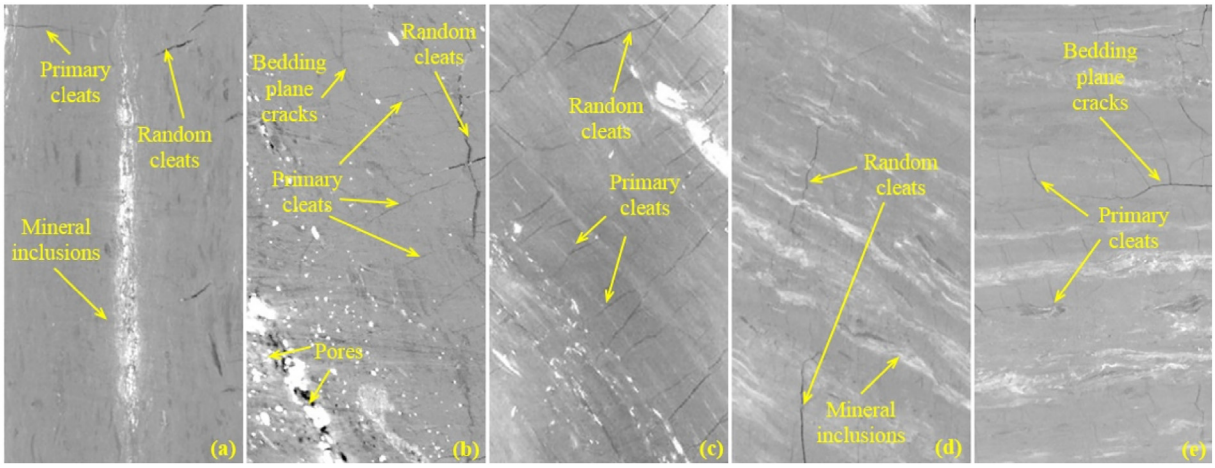

Fig. 2. Cross sections of coal samples with different anisotropic angles: (a) 0°; (b) 30°; (c) 45°; (d) 60°; (e) 90.

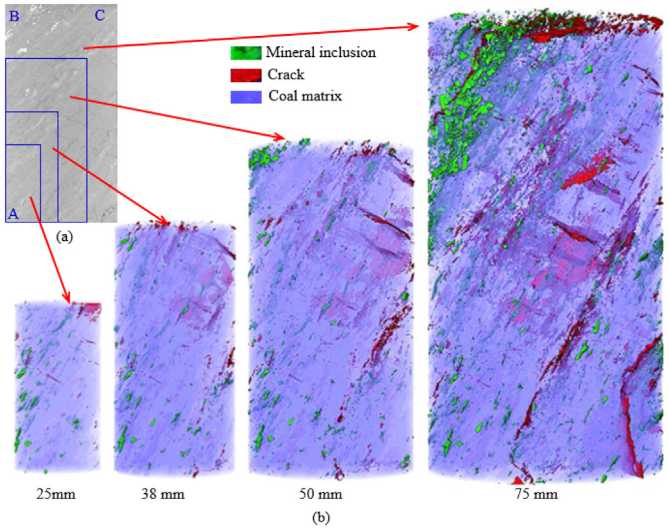

Fig. 3. Coal samples cropped from the specimen with a diameter of 75 mm and anisotropic angle of 45° and the variation of microstructures with increasing of specimen size: (a) Schematic diagram of image segmentation for groups A, B, and C; (b) Variation of microstructures with increasing specimen size in group A.

planes and bedding plane interfaces may be more pronounced than in coal.

4.2. Uniaxial compressive strengths

The mean value of UCS for specimens with different inclinations of anisotropy and size are summarized in Table 2, and Fig. 4. The curves of anisotropy versus UCS exhibit a U-shaped form, based on the classification of Ramamurthy (1993). For groups with different specimen sizes, the maximum UCS strengths are observed at $\beta = 90°$, and the second largest value at $\beta = 0°$, similar to that in other rocks. Minimum strengths occur at between 37° and 38°, which are higher than that for typical sedimentary rocks. This is due to the lower strength of coal matrix relative to indurated rocks, and that friction coefficient along the weakness is also smaller than that in rock materials (Zhao et al., 2014a, 2014b). For specimens in each orientation, the declination of the average UCS is the most obvious when the angle of anisotropy is 0°, with a reduction of 4.13 MPa as the specimen diameter increases from 25 mm to 75 mm, while it is a minimum at 45°, with a reduction of 2.66 MPa.

The strength anisotropy can be explained by the variation of microstructures in coal. The strength-anisotropy curves have a U-shaped form and this is due to the orientation of the weakness plane, formed by the microstructures (Fig. 2). When the angle of anisotropy is 0°, the occurrence of pre-existing cracks and mineral inclusions with the increasing specimen volume has a greater influence on the cohesive strength of the coal sample. Specimen strength is most sensitive to a weakness plane oriented parallel to the loading direction (Tavallali and Vervoort, 2010), as apparent from Fig. 2(a). The minimum failure strength is close to (45°-φ/2) as apparent in Fig. 2(c) (Cho et al., 2012),

Table 1
The volume variation of mineral inclusions and initial cracks in specimens with different diameters.

Diameter (mm)	Group	Mineral inclusions			Pre-existing cracks		
		Volume (mm^3)	Average volume (mm^3)	Variation (%)	Volume (mm^3)	Average volume (mm^3)	Variation (%)
25 mm	A	27.46	219.31	104.30	2.41	14.52	97.49
	B	518.67			21.46		
	C	84.70			35.72		
38 mm	A	191.22	408.08	100.76	153.61	115.76	58.13
	B	1076.62			257.55		
	C	352.11			385.50		
50 mm	A	594.33	476.92	83.80	354.22	185.48	48.49
	B	1357.69			492.98		
	C	324.42			682.86		
75 mm	A	3254.43	–	–	1456.08	–	–

Table 2
Uniaxial compression test results of coal samples with different sizes and loading directions.

Angle (°)	0		15		30		45		60		90		Average	
D (mm)	UCS (MPa)	Deviation (MPa)	UCS (MPa)	Deviation (MPa)	UCS (MPa)	Deviation (MPa)	UCS (MPa)	Deviation (MPa)	UCS (MPa)	Deviation (MPa)	UCS (MPa)	Deviation (MPa)	UCS (MPa)	Deviation (MPa)
25	16.01	7.75	15.12	8.00	13.23	3.86	13.19	2.63	14.51	5.34	17.52	1.63	14.93	5.64
38	14.30	3.89	13.48	2.79	11.78	2.01	11.80	2.21	13.09	3.81	15.85	1.46	13.38	3.17
50	12.79	2.12	12.41	3.02	11.16	1.18	11.22	0.93	11.94	3.19	14.36	1.26	12.31	2.40
75	11.88	1.55	11.62	3.03	10.43	0.99	10.53	0.45	11.30	2.24	13.44	0.26	11.53	2.01

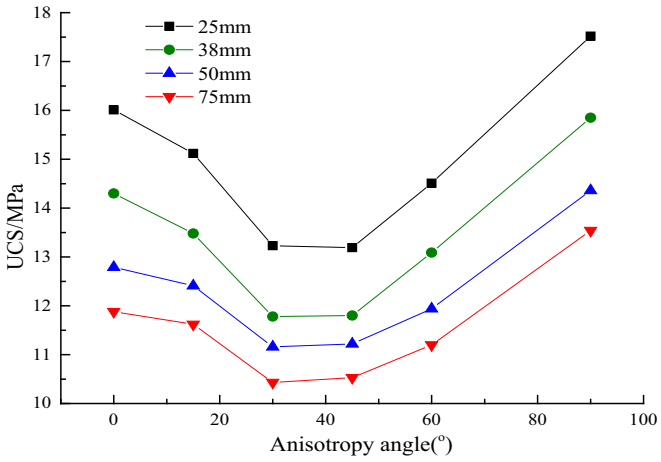

Fig. 4. Curves of strength anisotropy versus anisotropic angle in coal samples with different sizes.

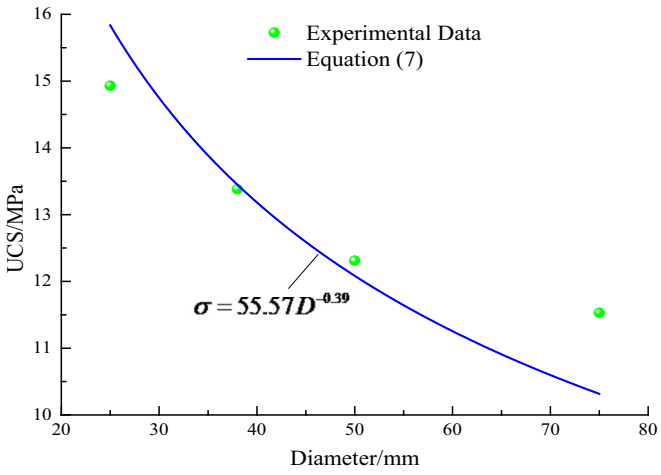

Fig. 5. Fitting result of Eq. (7) based on the experimental data obtained by this investigation.

as aided by the effect of microstructures.

At the same time, the degree of strength anisotropy reduces as the specimen size increases. This is apparent in the standard deviation of the average UCS that reduces from 5.64 MPa to 2.01 MPa as the specimen diameter increases from 25 mm to 75 mm. This is principally due to the enhanced microstructural volume of a larger specimen, see Table 1 and Fig. 2.

4.3. Scale effect on coal strength

Based on theory, the foregoing experimental data and empirical equations relating to scale effects, three principles defining this response are as follows:

1. The relationship between the specimen size and UCS is dependent on the mechanical properties of the material;
2. Specimen size is negatively correlated with the UCS;
3. For specimens of a prescribed shape, the UCS of the coal (and other rock materials) is constant for specimens either larger or smaller than threshold sizes.

To evaluate the applicability of the foregoing equations relating specimen size to the UCS of coal, Eqs. (3) and (5) are used to fit the experimental data obtained in this investigation.

A transferred form of Eq. (3) was used to make it suitable for cylindrical specimens, as width to height ratio is constant, and the new equation can be expressed as

$$\sigma = Cw^{-0.39} \quad (7)$$

where σ is the specimen strength, MPa; w is the sample width, mm; and C is a constant, determined by material and specimen shape. In this case C is obtained by fitting Eq. (7) to the experimental data. Eq. (7) may have disadvantages in describing the variation of the UCS with the specimen size, since the UCS is close to 0 when specimen is infinitely large. Thus this relation must have a threshold minimum when the specimen size is greater than a critical value (Bieniawski, 1968a). Thus, the discrepancy of Eq. (7) to the experimental data will occur when the specimen size is greater than the threshold size.

Fig. 5 illustrates that the discrepancy in curve fitting to the experimental data of Eq. (7) appears and becomes apparent when specimen diameter is greater than ~60 mm, despite numerous curve fitting parameters were attempted. Meanwhile, it also indicates the range of the specimen diameter in this research is wide enough to define this region of contradictory results between the theoretically predicted UCS of Eq. (7) and the experimental data. Notably, Eq. (5) fits well when the specimen size is > 50 mm but fails when the specimen diameter is smaller than 50 mm (Fig. 6).

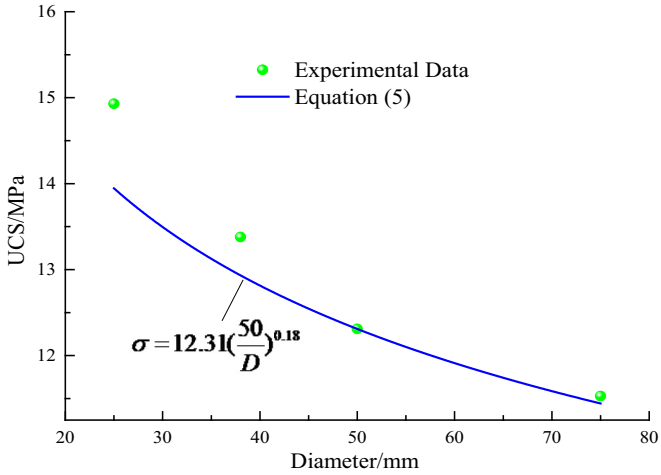

Fig. 6. Comparison of Eq. (5) and the experimental data in this paper.

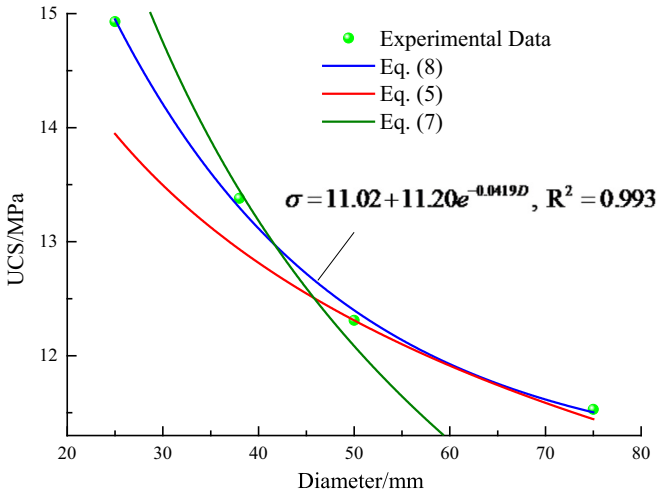

Fig. 7. Regression analysis result of Eq. (8) and comparison of Eq. (8), and Eqs. (5) and (7).

Clearly, Eqs. (1)–(5) incorporate the principles summarized above, to some extent, while the fit curves in Figs. 5 and 6, and the aforementioned investigation (Bieniawski, 1968a) indicates that difficulties exist in using these equation in coal samples.

Thus, a new empirical formula is developed to reveal the relationship between specimen size and the UCS that can be used in coal specimens with a prescribed width to height ratio. Any such relations should have two parts. The first is constant that represent the UCS when the specimen length or diameter $d \rightarrow \infty$, namely σ_M; and a second part is a function that can represent the reduction in the UCS as the specimen size increases from 0 to ∞. Thus, this formula should have the form

$$\sigma_d = \sigma_M + (\sigma_0 - \sigma_M)e^{-kd} \quad (8)$$

where σ_d is the strength of the coal sample when specimen diameter is d; σ_0 is the UCS when $d \rightarrow 0$; k is related to the mechanical properties of the coal sample. The values of σ_M and σ_0 are related to mechanical properties and loading conditions of the coal specimen, and k, σ_M and σ_0 can be obtained from the fitting result, based on a series of uniaxial compressive tests on coal specimen of different sizes and loading directions.

Eq. (8) is verified by these experimental data, as shown in Fig. 7 (correlation coefficient of 0.993). Based on this fitting result, the parameter k is 0.0042, and σ_M and σ_0 are 11.02 MPa and 22.22 MPa, respectively. Meanwhile, Eq. (8) is also compared with other previously well-recognized equations on scale effect in coal and rock, namely Eqs. (7) and (5), in Fig. 7. The comparison reveals that Eq. (8) has advantages in describing the effect of specimen size on the variation of UCS and better reflects the variation of the experimental data with specimen diameters than the other two formulae.

To verify the applicability of Eq. (8) on coal samples with different shapes and mechanical properties, data on cubical specimen obtained by Bieniawski in South Africa (Bieniawski, 1968a) and Gonzatti with smaples from Brazil (Gonzatti et al., 2014) are also used to verify the robustness of this empirical equation. The fitted results are shown in Fig. 8.

The curves in Fig. 8(a) and (b) fit well with the experimental data obtained by Bieniawski (1968a) and Gonzatti et al. (2014), and correlation coefficients (R^2) are > 0.93. This indicates that Eq. (8) can be used in coal specimens and also cubic samples and different coal types.

4.4. Anisotropic scale effect

The severity of the scale effect on the UCS varies with the angle of

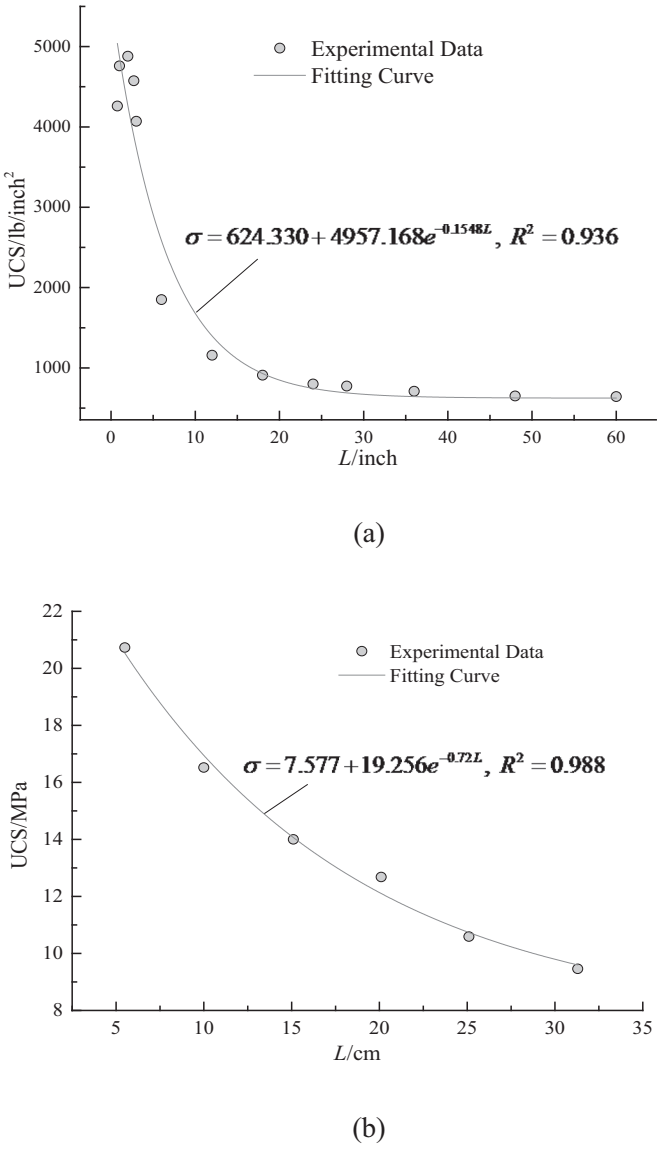

Fig. 8. The fitted curves of UCS with the length of cubic specimens, based on Eq. (8) and experimental data obtained by other researchers: (a) Coal samples from South African; (b) Coal samples from the South-Catarinense coalfield in Brazil.

anisotropy (Fig. 4). To evaluate the influence of anisotropy on the scale effect, Eq. (8) is used since σ_M and σ_0 change with the loading direction. The fitted result of Eq. (8) is shown in Fig. 9 and σ_m, σ_0, and k of Eq. (8) in every loading direction are summarized in Table 3.

Clearly, fitting curves in Fig. 9 agree well with the experimental data, and correlation coefficients of Eq. (8) are > 0.98. Thus, the UCS in each loading direction for specimen sizes approaching both 0 and ∞ is also predicted by Eq. (8), based on the σ_M, and σ_0 summarized in Table 3. When the specimen size approaches 0 and ∞, the maximum UCS magnitudes of coal are 26.49 MPa and 12.81 MPa, respectively, as the angle of anisotropy is 90°, while minimum values are 19.08 MPa and 10.02 MPa, respectively, when the anisotropic angle is 30°.

Accordingly, a comparison of the predicted data when the specimen diameter approaches either 0 or ∞ and experimental data of the UCS for specimen diameters of 25 mm, 38 mm, 50 mm, and 75 mm is plotted in Fig. 10. It is apparent that the strength anisotropy trend predicted by Eq. (8) accords well with the experimental data summarized in Table 2. As can be seen from Fig. 10, the anisotropic response of specimens with diameters approaching 0 and ∞ also exhibits a U-shape form with the

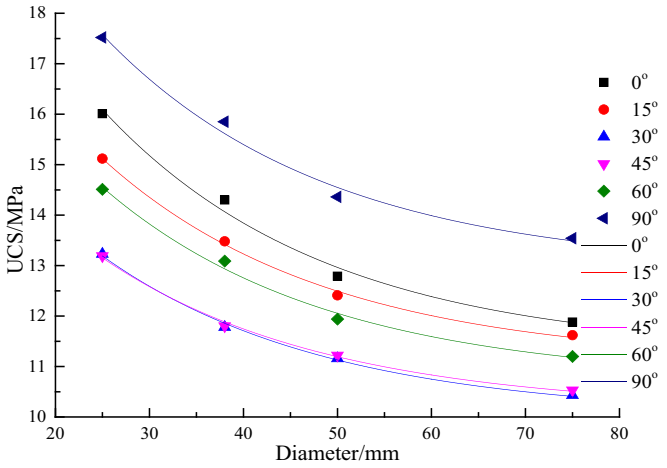

Fig. 9. The scale effect on the UCS of coal samples with different anisotropic angles.

Table 3
Parameters in Eq. (8) when the coal specimen is loaded in various directions.

Angle (°)	0	15	30	45	60	90
σ_m (MPa)	11.28	11.08	10.02	10.14	10.71	12.81
σ_0 (MPa)	25.03	22.62	19.08	19.25	21.69	26.49
σ_0–σ_m (MPa)	13.75	11.54	9.06	9.11	10.98	13.68
k	0.042					
R^2	0.986	0.997	0.997	0.996	0.995	0.980

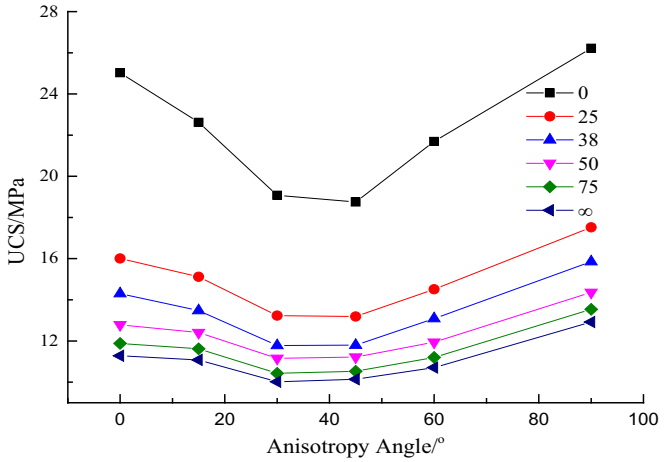

Fig. 10. Comparison of experimental data when specimen diameters are 25 mm, 38 mm, 50 mm, and 75 mm with theoretically predicted data obtained by Eq. (8) when the specimen diameter is close to 0 and approaches ∞.

minimum UCS at an anisotropic angle of ~30°–45°. The maximum UCS is reached at an angle of anisotropy of 90°, and the second largest UCS is at an anisotropic angle of 0°.

To compare the anisotropy of the scale effect on coal specimen strength, the derivative of Eq. (8) is

$$\sigma_d' = -(\sigma_0 - \sigma_M)ke^{-kd} \tag{9}$$

where σ_d' is the derivative of σ_d. Values of the derivative are negative, as (σ_0–σ_m) and k are positive. Based on σ_M, σ_0, (σ_0-σ_M), and k, summarized in Table 3. The derivative of σ_d' is a maximum value at 45°, and a minimum at 0°. Thus, the scale effect on coal strength is strongest when the angle of anisotropy is inclined at 0°, and is a minimum at 45°, when specimen diameter increase from 0 to ∞.

4.5. Anisotropy of coal strength with various specimen sizes

Compared with other sedimentary rock, more factors should be considered in the theoretical description of the strength variation in coal with the angle of anisotropy. This is due to the lower strength of the coal matrix (Zhao et al., 2014a), smaller differences between adjacent layers of the bedding planes, less pronounced effects of the bedding plane on the strength variation of coal samples with different inclinations of bedding planes (Nasseri et al., 2003; Pomeroy et al., 1971), and the significant influence of cleats that are orthogonal to the bedding plane. These features all influence the strength of coal (Pomeroy et al., 1971).

Eq. (6) is theoretically developed by Jaeger (1960), based on the continuous variation of cohesive resistance induced by changes in the angle between loading direction and bedding plane. Parameters in Eq. (6) reflect frictional, tensile or cohesive features of the rock whose anisotropic curves show a U-shaped form viz. $\beta_{min} = (45° - \varphi/2)$, where β_{min} is the orientation angle of the bedding plane that has minimum value of uniaxial compressive strength and φ is the frictional angle. Constants A and D in Eq. (6) also provides flexibility in considering the effect of other factors such as cleats that are perpendicular to the bedding plane, and are ubiquitous in various kinds of rocks. Thus, Eq. (6) is used in the regression analysis of the relationship between the UCS and the anisotropic angle of specimens of different sizes with β_{min} chosen as 37.5°, based on Fig. 10.

Fitting curves in Fig. 11 agree well with both the experimental and predicted data, and correlation coefficients (R^2) of Eq. (6) are > 0.87. Meanwhile, the value of parameters A and D in Eq. (6) decreases from 25.74 and 6.21 to 12.16 and 2.07, respectively, as the specimen diameter increases from 0 mm to ∞, as shown in Table 4.

Since parameter D in Eq. (6) is positively correlated with the variation of the range of UCS magnitudes, the declination of D in Table 4 indicates that the strength anisotropy in coal reduces with the increasing specimen size but will asymptote to a constant when the specimen size is larger than a critical threshold. This is consistent with the anticipated sense of the scale effect on coal strength and its variation with strength anisotropy as predicted by Eq. (8), as shown in Fig. 10.

Thus, Eq. (6) is applicable in describing the strength variation of coal with the anisotropic angle in different specimen sizes.

4.6. Universal equation for scale effects and strength anisotropy of coal

A unified equation describing the relationship among UCS, specimen size, and loading direction in coal is crucial for the correct estimation of strength size of the loaded feature. Since σ_0 and σ_M in Eq. (8) can be replaced by Eq. (6), a unified empirical equation describing both the scale effect and strength anisotropy in coal is proposed in the form

$$\sigma(d,\beta) = A_M - D_M \cos 2(\beta - \beta_{min}) + [(A_0 - A_M) - (D_0 - D_M)\cos 2(\beta - \beta_{min})]e^{-kd} \tag{10}$$

where d is the specimen diameter, mm; $\sigma(d, \beta)$ is the UCS of the coal specimen with a diameter d and the angle of anisotropy is β (°); A and D are constants as defined in Eq. (6), A_0 and D_0, A_M and D_M are the constants A and D when the sample is infinitely large (close to ∞) or vanishingly small (0), respectively; k is a positive constant related to mechanical properties of coal, as mentioned in Eq. (8); β_{min} is the anisotropy angle where the UCS is a minimum.

A comparison of experimental data and Eq. (10) is shown in Fig. 12. The regression result indicates that Eq. (10) is applicable in representing relations among specimen size, UCS, and loading direction. The theoretical surface obtained by Eq. (10) agrees well with the experimental data in Fig. 12, with all experimental data close to the theoretical surface and represented by a correlation coefficient (R^2) of 0.972.

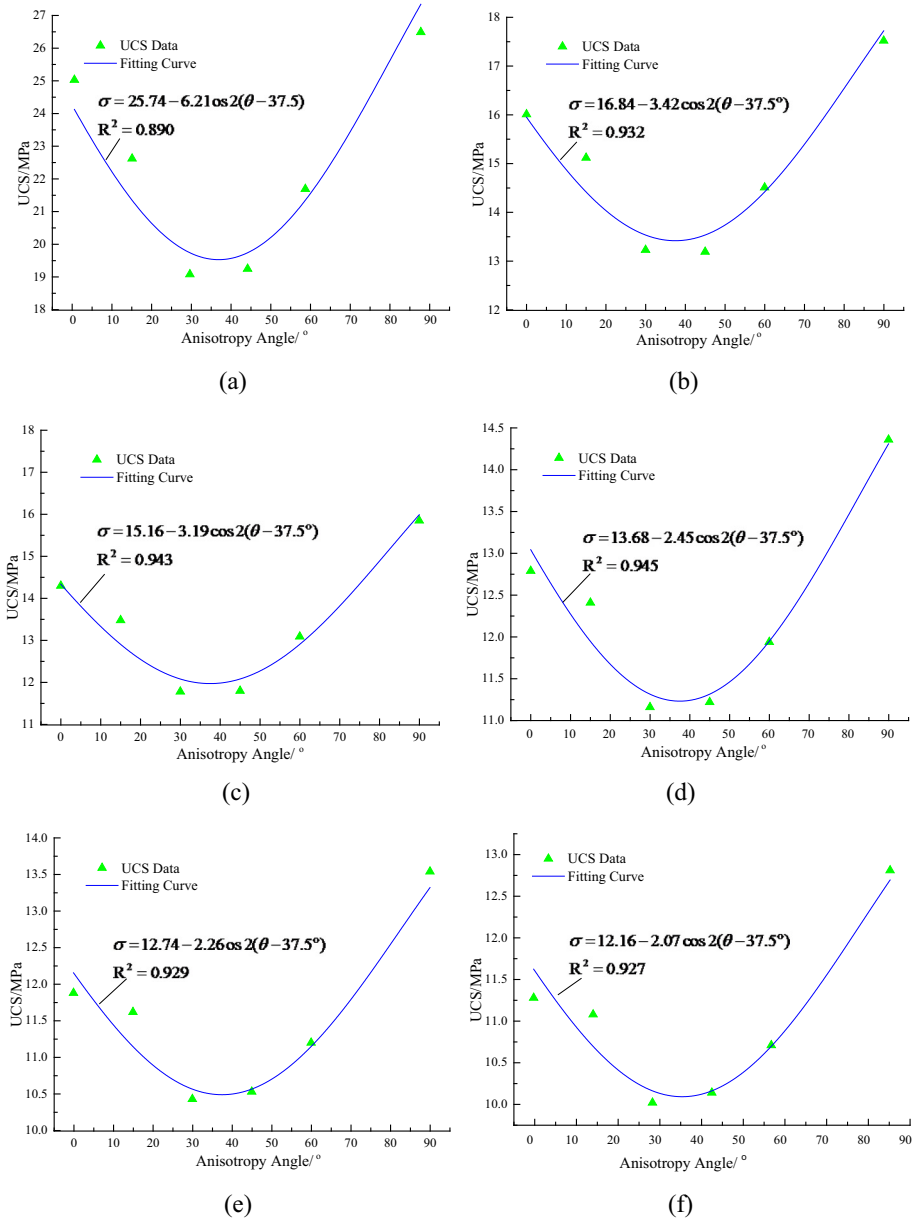

Fig. 11. Fitted curves of UCS versus anisotropic angles of coal specimens with different diameters, based on Eq. (6): (a) $d \rightarrow 0$; (b) $d = 25$ mm; (c) $d = 38$ mm; (d) $d = 50$ mm; (e) $d = 75$ mm; (f) $d \rightarrow \infty$.

Table 4
The variation of parameters A and B with the increasing of specimen sizes.

Diameter (mm)	d → 0	25	38	50	75	d → ∞
A	25.74	16.84	15.16	13.68	12.76	12.16
D	6.21	3.42	3.19	2.45	2.24	2.07
R^2	0.879	0.932	0.943	0.945	0.929	0.927

The utility of Eq. (10) is in providing an approach to obtain the coal specimen strength as both the specimen size and anisotropy vary. The drawback of Eq. (10) is that coal specimens of various sizes and anisotropy angles are needed to obtain parameters in Eq. (10) for each particular material. However, the characteristic properties of the angle of minimum strength, its magnitude at that orientation, and the Weibull distribution describing sample size are all combined to enable a mechanistic description of behavior.

5. Conclusions

Microstructure-related scale effects and strength anisotropy in coal are investigated, based on uniaxial compressive tests performed on a series of coal samples with different sizes and orientations of loading relative to anisotropy. These behaviors also draw on the role of the variation of microstructures with specimen size characterized by X-ray CT imaging. The conclusions are obtained as below:

1. The UCS in coal shows a U-shaped relation with the angle of loading relative to the anisotropy and for different sample sizes that similar to that obtained by Jaeger (1971). The degree of strength anisotropy decreases with increasing specimen size, due to the enhanced microstructural volume of a larger specimen. The rate of the declination of the average UCS with loading orientation is greatest when loading is parallel to bedding (anisotropy angle is 0°) and is least at 45°.
2. An empirical equation relating the UCS and specimen size is

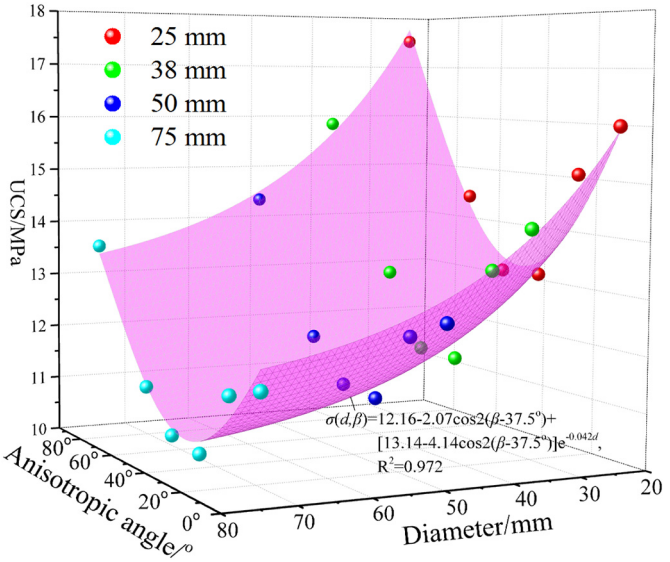

Fig. 12. Comparison of experimental data with a theoretical surface in specimens of various diameters, based on Eq. (10).

obtained and verified against experimental data. Based on this equation, the UCS is defined at the limiting conditions when the specimen is either very small (close to 0) or very large (∞), and for different orientations of the loading.

3. A cosine relation between angle of anisotropy and UCS is applicable in coal samples at different scales - the strength anisotropy remains constant for specimens larger than a critical size.
4. Based on the two relations developed in this work, a universal equation revealing the relationship among specimen size, anisotropy angle and UCS of coal and depending on the minimum strength angle, friction angle and Weibull coefficients of coal is proposed and verified against experimental data.

Acknowledgments

This research is supported by the National Key R&D Program of China (2016YFC0801401 and 2016YFC0600708), Yue Qi Distinguished Scholar Project of China University of Mining & Technology (Beijing) and Fundamental Research Funds for the Central Universities. We acknowledge the constructive comments of the editor and two anonymous reviewers that improved an earlier version of this paper.

References

Ajalloeian, R., Lashkaripour, G.R., 2000. Strength anisotropies in mudrocks. Bull. Eng. Geol. Environ. 59, 195–199. http://dx.doi.org/10.1007/s100640000055.
Al-Harthi, A.A., 1998. Effect of planar structures on the anisotropy of Ranyah sandstone, Saudi Arabia. Eng. Geol. 50, 49–57. http://dx.doi.org/10.1016/S0013-7952(97)00081-1.
Amadei, B., 1996. Importance of anisotropy when estimating and measuring in situ stresses in rock. Int. J. Rock Mech. Min. Sci. Geomech. Abstr. 33, 293–325. http://dx.doi.org/10.1016/0148-9062(95)00062-3.
Behrestaghi, M.H.N., Rao, K.S., Ramamurthy, T., 1996. Engineering geological and geotechnical responses of schistose rocks from dam project areas in India. Eng. Geol. 44, 183–201. http://dx.doi.org/10.1016/S0013-7952(96)00069-5.
Bieniawski, Z.T., 1968a. The effect of specimen size on compressive strength of coal. Int. J. Rock Mech. Min. Sci. Geomech. Abstr. 5, 325–335. http://dx.doi.org/10.1016/0148-9062(68)90004-1.
Bieniawski, Z.T., 1968b. In situ strength and deformation characteristics of coal. Eng. Geol. 2, 325–340. http://dx.doi.org/10.1016/0013-7952(68)90011-2.
Brook, N., 1985. The equivalent core diameter method of size and shape correction in point load testing. Int. J. Rock Mech. Min. Sci. Geomech. Abstr. 22, 61–70. http://dx.doi.org/10.1016/0148-9062(85)92328-9.
Cai, Y., Liu, D., Pan, Z., Yao, Y., Li, C., 2015. Mineral occurrence and its impact on fracture generation in selected Qinshui Basin coals: an experimental perspective. Int. J. Coal Geol. 150–151, 35–50. http://dx.doi.org/10.1016/j.coal.2015.08.006.
Chenevert, M.E., Gatlin, C., 1965. Mechanical anisotropies of laminated sedimentary rocks. Soc. Pet. Eng. J. 5, 67–77. http://dx.doi.org/10.2118/890-PA.
Cho, J.W., Kim, H., Jeon, S., Min, K.B., 2012. Deformation and strength anisotropy of Asan gneiss, Boryeong shale, and Yeoncheon schist. Int. J. Rock Mech. Min. Sci. 50, 158–169. http://dx.doi.org/10.1016/j.ijrmms.2011.12.004.
Cundall, P.A., Pierce, M.E., Mas Ivars, D., 2008. Quantifying the size effect of rock mass strength. 1st south. Hemisph. Int. Rock Mech. Symp. 15.
Deklotz, E.J., Brown, J.W., Stemler, O.A., 1966. Anisotropy of a Schistose Gneiss. 1st ISRM Congr. pp. 465–470.
Donath, F.A., 1961. Experimental study of shear failure in anisotropic rocks. GSA Bull. 72, 985–989.
Gao, F., Stead, D., Kang, H., 2014. Numerical investigation of the scale effect and anisotropy in the strength and deformability of coal. Int. J. Coal Geol. 136, 25–37. http://dx.doi.org/10.1016/j.coal.2014.10.003.
George, J.D.S., 1997. Structural effects on the strength of New Zealand coal. Int. J. Rock Mech. Min. Sci. 34, 299.e1–299.e11. http://dx.doi.org/10.1016/S1365-1609(97)00184-6.
Gonzatti, C., Zorzi, L., Agostini, I.M., Fiorentini, J.A., Viero, A.P., Philipp, R.P., 2014. In situ strength of coal bed based on the size effect study on the uniaxial compressive strength. Int. J. Min. Sci. Technol. 24, 747–754. http://dx.doi.org/10.1016/j.ijmst.2014.10.003.
Gregory, B., Herbert, E., 1981. Size effect in rock testing. Geophys. Res. Lett. 8, 671–674. http://dx.doi.org/10.1029/GL008i007p00671.
Heng, S., Guo, Y., Yang, C., Daemen, J.J.K., Li, Z., 2015. Experimental and theoretical study of the anisotropic properties of shale. Int. J. Rock Mech. Min. Sci. 74, 58–68. http://dx.doi.org/10.1016/j.ijrmms.2015.01.003.
Hoek, E., Brown, E.T., 1980. Underground Excavations in Rock. CRC Press, London.
Hoek, E., Brown, E.T., 1997. Practical estimates of rock mass strength. Int. J. Rock Mech. Min. Sci. 34, 1165–1186. http://dx.doi.org/10.1016/S1365-1609(97)80069-X.
ISRM, 2007. The complete ISRM suggested methods for rock characterization, testing and monitoring. Int. Soc. Rock Mech. Comm. Test. Methods 1974–2006.
Jaeger, J.C., 1960. Shear failure of anistropic rocks. Geol. Mag. 97, 65–72. http://dx.doi.org/10.1017/S0016756800061100.
Jaeger, J.C., 1971. Friction of rocks and stability of rock slopes. Géotechnique 21, 97–134. http://dx.doi.org/10.1680/geot.1971.21.2.97.
Jing, X.D., Al-Harthy, S., King, M.S., 2002. Petrophysical properties and anisotropy of sandstones under true-triaxial stress conditions. Petrophysics 43, 358–364.
Karacan, C.O., Okandan, E., 2001. Adsorption and gas transport in coal microstructure: investigation and evaluation by quantitative X-ray CT imaging. Fuel 80, 509–520. http://dx.doi.org/10.1016/S0016-2361(00)00112-5.
Karpyn, Z.T., Piri, M., 2007. Prediction of fluid occupancy in fractures using network modeling and x-ray microtomography. I: data conditioning and model description. Phys. Rev. E 76 (16315). http://dx.doi.org/10.1103/PhysRevE.76.016315.
Khanlari, G., Rafiei, B., Abdilor, Y., 2015. Evaluation of strength anisotropy and failure modes of laminated sandstones. Arab. J. Geosci. http://dx.doi.org/10.1007/s12517-014-1411-1.
Levine, J.R., Davis, A., 1984. Optical anisotropy of coals as an indicator of tectonic deformation, broad top coal field, Pennsylvania. GSA Bull. 95, 100–108.
Liu, S., Sang, S., Wang, G., Ma, J., Wang, X., Wang, W., Du, Y., Wang, T., 2017. FIB-SEM and X-ray CT characterization of interconnected pores in high-rank coal formed from regional metamorphism. J. Pet. Sci. Eng. 148, 21–31. http://dx.doi.org/10.1016/j.petrol.2016.10.006.
Mao, L., Hao, N., An, L., Chiang, F., Liu, H., 2015. 3D mapping of carbon dioxide-induced strain in coal using digital volumetric speckle photography technique and X-ray computer tomography. Int. J. Coal Geol. 147–148, 115–125. http://dx.doi.org/10.1016/j.coal.2015.06.015.
Mas Ivars, D., Pierce, M.E., Degagné, D., Darcel, C., 2008. Anisotropy and scale dependency in jointed rock-mass strength – a synthetic rock mass study. Contin. Distinct Elem. Numer. Model. Geo-Eng. 1–9.
Masoumi, H., Saydam, S., Hagan, P., 2015. Unified size-effect law for intact rock. Int. J. Geomech. 16, 1–15. http://dx.doi.org/10.1061/(ASCE)GM.1943-5622.0000543.
McLamore, R., Gray, K.E., 1967. The mechanical behavior of anisotropic sedimentary rocks. J. Eng. Ind. 89, 62–73.
Medhurst, T.P., 1997. Estimation of the In Situ Strength and Deformability of Coal for Engineering Design. The University of Queensland.
Medhurst, T.P., Brown, E.T., 1998. A study of the mechanical behaviour of coal for pillar design. Int. J. Rock Mech. Min. Sci. 35, 1087–1105. http://dx.doi.org/10.1016/S0148-9062(98)00168-5.
Nasseri, M.H.B., Rao, K.S., Ramamurthy, T., 2003. Anisotropic strength and deformational behavior of Himalayan schists. Int. J. Rock Mech. Min. Sci. 40, 3–23. http://dx.doi.org/10.1016/S1365-1609(02)00103-X.
Okubo, S., Fukui, K., Qingxin, Q., 2006. Uniaxial compression and tension tests of anthracite and loading rate dependence of peak strength. Int. J. Coal Geol. 68, 196–204. http://dx.doi.org/10.1016/j.coal.2006.02.004.
Pan, J., Meng, Z., Hou, Q., Ju, Y., Cao, Y., 2013. Coal strength and young's modulus related to coal rank, compressional velocity and maceral composition. J. Struct. Geol. 54, 129–135. http://dx.doi.org/10.1016/j.jsg.2013.07.008.
Pan, J., Wang, K., Hou, Q., Niu, Q., Wang, H., Ji, Z., 2016. Micro-pores and fractures of coals analysed by field emission scanning electron microscopy and fractal theory. Fuel 164, 277–285. http://dx.doi.org/10.1016/j.fuel.2015.10.011.
Pietruszczak, S., Lydzba, D., Shao, J.F., 2002. Modelling of inherent anisotropy in sedimentary rocks. Int. J. Solids Struct. 39, 637–648. http://dx.doi.org/10.1016/S0020-7683(01)00110-X.
Pomeroy, C.D., Hobbs, D.W., Mahmoud, A., 1971. The effect of weakness-plane orientation on the fracture of Barnsley Hards by triaxial compression. Int. J. Rock Mech. Min. Sci. Geomech. Abstr. 8, 227–238. http://dx.doi.org/10.1016/0148-9062(71)90021-0.

Poulsen, B.A., Adhikary, D.P., 2013. A numerical study of the scale effect in coal strength. Int. J. Rock Mech. Min. Sci. 63, 62–71. http://dx.doi.org/10.1016/j.ijrmms.2013.06.006.
Protodiakonov, M.M., Koifman, M.I., 1963. The scale effect in investigations of rock and coal. In: Proceedings of 5th Congress International Bureau Rock Mechanics, Leipzig.
Qi, C., Wang, M., Bai, J., Li, K., 2014. Mechanism underlying dynamic size effect on rock mass strength. Int. J. Impact Eng. 68, 1–7. http://dx.doi.org/10.1016/j.ijimpeng.2014.01.005.
Rafiai, H., 2011. New empirical polyaxial criterion for rock strength. Int. J. Rock Mech. Min. Sci. 48, 922–931. http://dx.doi.org/10.1016/j.ijrmms.2011.06.014.
Ramamurthy, T., 1993. Strength and modulus responses of anisotropic rocks. Compr. Rock Eng. 1 (1), 313–329.
Saeidi, O., Vaneghi, R.G., Rasouli, V., Gholami, R., 2013. A modified empirical criterion for strength of transversely anisotropic rocks with metamorphic origin. Bull. Eng. Geol. Environ. 72, 257–269. http://dx.doi.org/10.1007/s10064-013-0472-9.
Saroglou, H., Tsiambaos, G., 2008. A modified Hoek–Brown failure criterion for anisotropic intact rock. Int. J. Rock Mech. Min. Sci. 45, 223–234. http://dx.doi.org/10.1016/j.ijrmms.2007.05.004.
Scholtès, L., Donzé, F.-V., Khanal, M., 2011. Scale effects on strength of geomaterials, case study: coal. J. Mech. Phys. Solids 59, 1131–1146. http://dx.doi.org/10.1016/j.jmps.2011.01.009.
Shi, X., Pan, J., Hou, Q., Jin, Y., Wang, Z., Niu, Q., Li, M., 2018. Micrometer-scale fractures in coal related to coal rank based on micro-CT scanning and fractal theory. Fuel 212, 162–172. http://dx.doi.org/10.1016/j.fuel.2017.09.115.
Tavallali, A., Vervoort, A., 2010. Failure of layered sandstone under Brazilian test conditions: effect of micro-scale parameters on macro-scale behaviour. Rock Mech. Rock. Eng. 43, 641–653. http://dx.doi.org/10.1007/s00603-010-0084-7.
Van Belleghem, B., Montoya, R., Dewanckele, J., Van Den Steen, N., De Graeve, I., Deconinck, J., Cnudde, V., Van Tittelboom, K., De Belie, N., 2016. Capillary water absorption in cracked and uncracked mortar - a comparison between experimental study and finite element analysis. Constr. Build. Mater. 110, 154–162. http://dx.doi.org/10.1016/j.conbuildmat.2016.02.027.
Vega, B., Dutta, A., Kovscek, A.R., 2014. CT imaging of low-permeability, dual-porosity systems using high X-ray contrast gas. Transp. Porous Media 101, 81–97. http://dx.doi.org/10.1007/s11242-013-0232-0.
Vogel, H.-J., Cousin, I., Ippisch, O., Bastian, P., 2005. The dominant role of structure for solute transport in soil: experimental evidence and modelling of structure and transport in a field experiment. Hydrol. Earth Syst. Sci. Discuss. 2, 2153–2181. http://dx.doi.org/10.5194/hessd-2-2153-2005.
Wagner, H., 1974. Determination of the complete load-deformation characteristics of coal pillars. In: Proceedings of the Third International Congress on Rock Mechanics. National Academy of Sciences, pp. 1076–1081.
Ward, C.R., 2016. Analysis, origin and significance of mineral matter in coal: an updated review. Int. J. Coal Geol. 165, 1–27. http://dx.doi.org/10.1016/j.coal.2016.07.014.
Weibull, W., 1939. A Statistical Theory of the Strength of Materials. Ing. Vet. Ak. Handl.
Weibull, W., 1951. A statistical distribution function of wide applicability. J. Appl. Mech. 18 (3), 293–297. https://doi.org/citeulike-article-id:8491543.
Zhao, Y., Liu, S., Zhao, G.-F., Elsworth, D., Jiang, Y., Han, J., 2014a. Failure mechanisms in coal: dependence on strain rate and microstructure. J. Geophys. Res. Solid Earth 119, 6924–6935. http://dx.doi.org/10.1002/2014JB011198.
Zhao, Y., Zhao, G.F., Jiang, Y., Elsworth, D., Huang, Y., 2014b. Effects of bedding on the dynamic indirect tensile strength of coal: laboratory experiments and numerical simulation. Int. J. Coal Geol. 132, 81–93. http://dx.doi.org/10.1016/j.coal.2014.08.007.
Zhao, Y., Gong, S., Hao, X., Peng, Y., Jiang, Y., 2017. Effects of loading rate and bedding on the dynamic fracture toughness of coal: laboratory experiments. Eng. Fract. Mech. 178, 375–391. http://dx.doi.org/10.1016/j.engfracmech.2017.03.011.